

## Separation of Photogenerated Radical Ion Pairs in Viscous Solutions

A. I. Burshtein\* and A. A. Neufeld

Department of Chemical Physics, Weizmann Institute of Science, Rehovot 76100 Israel

Received: July 11, 2001; In Final Form: August 27, 2001

Encounter theory is used for the comparative study of two geminate reactions of backward electron transfer (recombination), followed by photoinduced bimolecular forward transfer. The latter can be affected by the initial correlations between similarly charged reactants, but a proper account of the electrostatic interactions shows that they are not responsible for the contrasting viscosity dependence of the recombination efficiency in these reactions. Instead, the observed qualitative difference in the experimental results is attributed to a parallel change of refraction index and dielectric constant in the solvent mixtures used for the viscosity variation in one of the reacting systems. Also it is demonstrated that neither the contact nor exponential models of transfer rates allow us to explain the nonmonotonic viscosity dependence of recombination efficiency, only the true Marcus' expression for the rates provides the explanation.

### I. Introduction

The separation of Radical Ion Pairs (RIPs), produced by electron or hole transfer from photoexcited donors to acceptors during their encounters in liquid solutions, is the subject of numerous experimental and theoretical investigations.<sup>1,2</sup> For a very long time the separation quantum yield,  $\bar{\alpha}$ , was estimated by the simplest formula of the so-called exponential model (EM):

$$\bar{\alpha}(\hat{\sigma}) = \frac{1}{1 + Z/\tilde{D}} \quad (1.1)$$

Here  $\tilde{D}$  is the coefficient of encounter diffusion separating the radical ion pairs and  $Z$  is the efficiency of their geminate recombination. In EM  $Z$  is determined solely by the rate of backward electron transfer (recombination), which does not depend on  $\tilde{D}$ . Later on it was shown that  $Z$  is really a constant, provided that both the forward and backward transfer occurs at the closest approach distance  $\hat{\sigma}$ ; i.e., ion pairs are born in contact and recombine there also.<sup>2,3</sup>

However, this is rarely the case. In general, the electron transfer occurs with the Marcus type rate  $W(r)$  at any given distance  $r$  between excited donor and acceptor.<sup>4</sup> The products of the forward transfer are generated farther apart, the slower the reactants approach each other. Their normalized distribution  $f(r)$  constitutes the initial conditions for backward electron transfer and diffusional separation of the ion pairs. Such an initial distribution of RIPs first introduced in the Unified Theory (UT) of forward and backward electron transfer<sup>5,6</sup> was studied a number of times.<sup>7–10</sup> A similar definition for this distribution was given in the newly developed Integral Encounter Theory (IET).<sup>11–13</sup> Both UT and IET operate with a charge separation yield  $\bar{\alpha}$ , which is actually the average of the partial yield  $\alpha(r)$  over initial distribution of starting distances:<sup>8,14,15</sup>

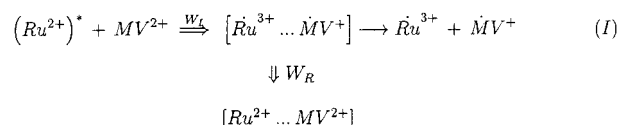
$$\bar{\alpha} = \int \alpha(r) f(r) d^3r \quad (1.2)$$

It is very important how the radical-ion distributions are positioned relative to the recombination layer, which can be either adjacent to contact or slightly shifted out of it. The

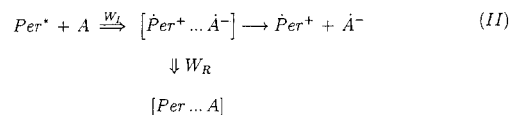
recombination inside this layer competes with radical ion separation, the more successfully the larger fraction of RIPs attends it, and the longer is their residence time in there. Both these factors depend on where the RIPs start, from inside or outside the recombination layer, and how fast they move to and through the layer. As a result the average charge separation quantum yield crucially depends on the shape of  $f(r)$  determined by the rate of forward electron transfer  $W_f(r)$  and the encounter diffusion of reactants. The latter changes with solvent viscosity, which usually is varied by using different solvents or solvent mixtures.

The short range wing of initial distribution represents the fraction of ions starting from inside the remote recombination layer. It is reasonably large at fast diffusion, but decreases when diffusion declines, so that at high viscosity all ions enter recombination layer from outside. For fast diffusion (inner starts) and slow diffusion (outer starts) the opposite diffusional dependence of the recombination efficiency was predicted.<sup>16</sup> What is  $Z(\tilde{D})$  in reality should be established experimentally.

Unfortunately, there are only two systems studied so far in solvents of different viscosity: ruthenium complex quenched by methyl viologen ( $MV^{2+}$ ), according to the reduced reaction scheme<sup>17</sup>



and perylene (Per) quenched by some aromatic amines (A):<sup>15,18</sup>



These systems differ in several aspects. In (I) the excitation participating in the forward transfer is triplet, while in (II) it is the singlet excited state; the electron transfer in reaction I occurs

between positively charged reactants, while in reaction II they are neutral for forward transfer and oppositely charged for backward transfer. Also, there is a pronounced difference in free energies (Figure 1). In reaction I both forward and backward electron transfer are less exergonic than in reaction II.

One or a combination of the aforementioned factors could be responsible for a qualitative difference in the diffusional dependence of  $Z$  in reactions I and II obtained in refs 17 and 15, respectively (Figure 2). In accordance with theoretical expectations,<sup>15</sup> the recombination efficiency in reaction II increases with diffusion in highly viscous solvents but decreases in solvents of low viscosity. However, in reaction I studied only in low viscosity solvents the behavior of  $Z$  is quite the opposite: it monotonically increases with diffusion. Earlier, this phenomenon was attributed to the diffusional delivery of remote RIPS to the contact recombination zone.<sup>19,20</sup> Here this explanation will be reconsidered and rejected, because neither the RIPS photogenerated in nonviscous solutions are remote, nor is the recombination zone contact at electron-transfer exergonicities peculiar to reaction I. To explain the difference between reactions I and II, the different energetics of electron transfer should be accounted for in conjunction with the macroscopic properties of solvent mixtures varying together with their viscosity.

An overview of the paper is as follows. In the next section we will present our input data, which are the simplest Marcus rates of forward and backward electron transfer, their free energy and space dependence. In section III the necessary extension of conventional encounter theory will be made to take into account the electrostatic interaction of reactants in solvents of different polarity and ionic strength. In section IV initial correlations are also included in the integral encounter theory used hereafter for all numerical investigations. First of all, the effect of Coulombic forces acting in reaction I was estimated in section V and recognized as unessential at relatively high ionic strength. Then in section VI the charge separation quantum yield is calculated with contact and exponential simplification of the transfer rates, as well as with their generic definitions. Finally, in section VII we take into account the systematic change of reorganization energy in solvent mixtures that accompanies their viscosity variation. This phenomenon is mainly responsible for the observed difference between the two reactions, as will be stressed again in the Conclusions.

## II. Description of the Model

In the case of a single-channel (“outer-sphere”) electron transfer, the rate of the forward transfer is given by the simplest Marcus formula:<sup>2</sup>

where  $\hat{i}(r)$  is the reorganization energy of electron transfer,  $w_i = V_i^2 \sqrt{\hat{\sigma}} / \sqrt{Ti(\hat{\sigma})}$  and  $L$  is a decay parameter of the tunneling matrix element, which equals  $V_i$  at contact distance  $\hat{\sigma}$ . The free energy of ionization is

where  $I$  and  $A$  are the ionization potential and electron affinity of the reaction partners, while  $\Delta U(r)$  is the difference in their electrostatic interaction before and after forward electron transfer.

The shape of the recombination reaction layer is given by the expression similar to (2.1)

where the preexponential factor  $w_r$  is the same as  $w_i$ , but for the backward electron transfer. The relative strength and space location of the forward and backward electron-transfer rates are mainly determined by the corresponding free energies,  $\Delta G_1(r)$  and  $\Delta G_R(r)$ , whose contact values are  $\Delta G$

The contact value of the last term  $\dot{\mathbf{i}}_0 = (e^2/\delta)\zeta$  is half as much as at infinite separation of reactants and is determined by Pekar's factor

$$\zeta = \left( \frac{1}{n^2} - 1 \right) \quad (2.7)$$

Both static dielectric constant and the refraction index  $n$  are changed together with the viscosity of solvent mixtures when their composition is varied.

### III. Initial Correlations

In conventional encounter theory, as well as in UT, the density of the primary excited molecules obeys the rate equation<sup>2</sup>

$$\dot{N} = -k_1(t)cN - \frac{N}{\delta} \quad (3.1)$$

where  $\delta$  is the lifetime of this state and  $c$  is the concentration of reaction partners, which is constant when the latter is present in great excess. The time dependent rate constant

$$k_1(t) = \int W_1(r) n(r,t) d^3r = -\int \dot{n}(r,t) d^3r \quad (3.2)$$

is expressed through the reactant distribution in the encounter pair  $n(r,t)$ . The latter obeys the auxiliary differential equation, with reflecting boundary conditions at the contact distance:

$$\dot{n} = -W_1(r)n + D \frac{\partial}{\partial r} r^2 e^{-U(r)/T} \frac{\partial}{\partial r} e^{U(r)/T} n \quad (3.3)$$

where the Boltzman constant  $k_B = 1$ ,  $D$  is the encounter diffusion coefficient for reactants, and  $U$  is the standard Debye–Hückel potential, which is zero for reaction II:

$$U = \begin{cases} \frac{q_1 q_2 e^2}{r(1 + \delta/\dot{\mathbf{i}}_D)} e^{-(r-\delta)/\dot{\mathbf{i}}_D} & \text{for reaction I} \\ 0 & \text{for reaction II} \end{cases} \quad (3.4)$$

Here  $q_1$  and  $q_2$  are the ion charges in units of electron charge  $e$ , and the so-called Debye screening length,

$$\dot{\mathbf{i}}_D = \sqrt{\frac{T}{4\delta e^2 n_e}} \quad (3.5)$$

is determined by the number density of ions  $n_e$ .

When there is no reaction, the stationary distribution of reactants is an equilibrium one,  $n_{\text{eq}} = g(r)$ , which is evidently an eigenfunction of a diffusional operator:

$$g = e^{-U(r)/T} \quad (3.6)$$

Due to electrostatic repulsion between reactants, the equilibrium distribution in (I) is not homogeneous, as in (II). The density of reacting ions is smaller when in contact than when farther away. This property is transferred to the initial distribution that arises after instantaneous light excitation at  $t = 0$ :

$$n(r,0) = g(r) \quad (3.7)$$

It is qualified as the ‘‘initial correlation’’ between reactants.

If  $W_1 \neq 0$  the electron-transfer results in nonexponential decay of the excitation survival probability, which is a solution of eq 3.1:

$$N(t) = N(0) \exp\left(-\frac{t}{\delta} - c \int_0^t k(t') dt'\right) \quad (3.8)$$

The initial value of the time dependent rate constant,

$$k_1(0) = \int W_1(r') g(r') d^3r' = k_0 \quad (3.9)$$

coincides with a true kinetic rate constant  $k_0$ , which takes into account the equilibrium inhomogeneity of the charged reactant around each other.

Such an inhomogeneity may be produced not only by partners interaction, but also by the liquid structure. The latter is determined by the reactant's surroundings, composed from the solvent molecules packed in the few nearest shells. It is reflected in the quasi-periodic structure of the pair correlation function at short distances, which is specific to both reacting systems under consideration. This structure is the short range factor that was studied thoroughly in a number of papers by Fayer's group.<sup>21</sup> However, in our present study it will be ignored together with the space dependence of  $\dot{\mathbf{i}}(r)$  and  $D(r)$ . These two factors analyzed in ref 22 were recognized as insignificant for fitting the theory to the whole experimentally studied kinetics of ion pair recombination. The quantum yield of their separation should be even less affected because the majority of ions that escape geminate recombination were born far from the contact. On the contrary, the space dependence of  $\dot{\mathbf{i}}$  and  $D$  is the most pronounced in near-contact, which is cut from the integrand of (1.2) by a multiplier,  $\bar{\alpha}(r)$ , having a dip there.

### IV. Integral Encounter Theory

Instead of unified theory we are using here the integral encounter theory, which is more fundamental<sup>12,13</sup> and simpler in quantum yield calculations.<sup>23–29</sup> The kinetics of geminate ion accumulation and recombination is described in IET by the following set of integro-differential equations:<sup>23</sup>

$$\dot{N}(t) = -c \int_0^t R^*(\delta) N(t-\delta) d\delta - \frac{N(t)}{\delta} \quad (4.1a)$$

$$\dot{P}(t) = c \int_0^t R^\dagger(\delta) P(t-\delta) d\delta \quad (4.1b)$$

The initial conditions for them are created by instantaneous light excitation at  $t = 0$ :

$$N(0) = N_0 \quad P(0) = 0$$

The kernels  $R^*$  and  $R^\dagger$  are given by their Laplace transformations  $\tilde{R}(s) = \int_0^\infty R(t) e^{-st} dt$ :

$$\tilde{R}^*(s) = \left(s + \frac{1}{\delta}\right) \int W_1(r) \tilde{\mathbf{I}}(r;s) d^3r \quad (4.2a)$$

$$\tilde{R}^\dagger(s) = \left(s + \frac{1}{\delta}\right) \int [W_1(r) \tilde{\mathbf{I}}(r;s) - W_R(r) \tilde{\mathbf{I}}(r;s)] d^3r \quad (4.2b)$$

The former accounts for the irreversible forward electron transfer, while the latter takes into account in addition the recombination of RIPs to the ground state. Both kernels are expressed via the Laplace transformation of the pair correlation functions  $\tilde{\mathbf{I}}$  and  $\tilde{\mathbf{I}}$ , which obey the auxiliary equations:

$$\left[s + \frac{1}{\delta} + W_1 - \mathcal{L}_r\right] \tilde{\mathbf{I}}(r;s) = g(r) \quad (4.3a)$$

$$[s + W_R - \mathcal{L}_r] \tilde{\mathbf{I}}(r;s) = W_1 \tilde{\mathbf{I}}(r;s) \quad (4.3b)$$

(with reflecting boundary conditions at  $r = \delta$ ). The linear operators

$$\mathcal{L}_r = \frac{1}{r^2} \frac{\partial}{\partial r} r^2 D(r) \left[ \frac{\partial}{\partial r} + \frac{1}{T} \frac{dU(r)}{dr} \right] \quad (4.4a)$$

$$\mathcal{L}_r^* = \frac{1}{r^2} \frac{\partial}{\partial r} r^2 \tilde{D}(r) \left[ \frac{\partial}{\partial r} + \frac{1}{T} \frac{dU'(r)}{dr} \right] \quad (4.4b)$$

represent the diffusion of reactants and reaction products in the corresponding electrostatic potentials,  $U$  and  $U'$ . The initial correlations between charged reactants participating in bimolecular forward electron transfer are represented in eq 4.3a by their initial equilibrium distribution  $g(r)$  defined in eq 3.7.

In the integral theory the desired charge separation quantum yield is expressed as the ratio of two kernels:<sup>23</sup>

$$\bar{\alpha} = \frac{\tilde{R}^{\ddagger}(0)}{R^*(0)} \quad (4.5)$$

They can be calculated directly from their definitions (4.2) for any given transfer rates  $W_f(r)$ ,  $W_R(r)$  and potentials  $U(r)$ ,  $U'(r)$  provided the set of equations (4.3) and (4.3b) is solved. This is much easier to do than to calculate the complete recombination kinetics  $P(t)$  from which we need only its asymptotic value  $\bar{\alpha} = P(\infty)$ . Alternatively, the quantum yield could be found from eq 1.2 provided both multipliers in the integrand are first calculated separately and only then averaged together. Unfortunately, one of them,  $\alpha(r)$ , is again the long time asymptotic value of partial survival probability, which is not easier to find than its averaged value.

As far as we know there are only a few precedents of studying the time evolution of survival probability in nonzero Coulombic potential.<sup>30</sup> Due to complexity of the problem, the account was never made for initial correlations as well as for the screening effect. Since all such details are essential for charged reactants in (I), one needs a much simpler approach to quantum yield calculation.

It is provided by only integral encounter theory. The latter reduces the problem to analytic or numerical calculation of two kernels in eq 4.5, thus avoiding the more complex solution of kinetic equations, either differential or integral. In contact approximation the kernels are available for even analytic calculations. They have been already obtained and used for the analysis of the Stern–Volmer constant<sup>31</sup> and charge recombination to either the ground or excited state of transfer products.<sup>32</sup> Since for the present goal the contact approximation is insufficient, we will use instead the original numerical program that has been already presented itself in a good light.<sup>32</sup> It allows us to specify the kernels at any given rate of remote electron transfer.

## V. Effect of the Coulombic Forces

As mentioned in the Introduction, both the forward and backward electron transfer in reaction I occur between positively charged reactants, while in reaction II the forward electron transfer proceeds between neutral reactants, while the backward one involves oppositely charged species. The difference between the two reactions is insignificant in highly polar solvents ( $\epsilon \rightarrow \infty$ ), but in less polar solution the effect of the Coulombic forces should be accounted for and analyzed in more detail.

Reaction I was conducted in ionic solutions, when an electrolyte is dissolved in an inert solvent, like acetonitrile, etc. The electrostatic interaction between reactants in such a system defined in eq 3.4, strongly depends on the ionic strength of the solution  $\hat{I}$  (mol/L). The latter determines the Debye screening length  $\hat{\lambda}_D$ , expressed through the number density of ions (number

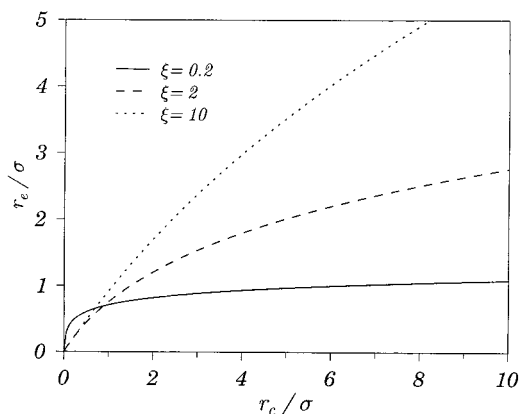


**Figure 3.** Effective distance of the Debye–Hückel potential  $r_e$ , in units of contact radius, against the Onsager length in the same units at different values of the dimensionless parameter  $E = r_c / \lambda_D$ , characterizing the efficiency of screening in eqs 5.3 and 5.5.

of electrons per  $\text{cm}^3$ ),

$$n_e = 2N_A \hat{I} / 1000 \quad (5.1)$$

where  $N_A$  is Avogadro's number. As follows from eqs 3.5 and 5.1, at room temperature ( $T = 293$  K) one has

$$\hat{\lambda}_D = 1.065 \sqrt{\hat{I}} \text{ \AA} \quad (5.2)$$

In the simplest models of charge separation the screening is neglected and the Coulomb potentials are represented as  $\pm r_c / r$ , where the sign is positive for electrostatic repulsion and negative for attraction. The Onsager radius  $r_c = q_1 q_2 e^2 / (T)$  is the distance, where the Coulombic potential becomes equal to the mean heat energy of the surrounding media. By this analogy we introduce the effective distance  $r_e$  of the screened potential (3.4) as  $|U(r_e)| = T$ , which gives

$$\frac{r_e}{\sigma} = E W_L \left[ \frac{r_c}{\sigma} \frac{e^{1/E}}{(1+E)} \right] \quad E = \frac{\hat{\lambda}_D}{\sigma} \quad (5.3)$$

where  $W_L$  is the Lambert  $W$  function.<sup>33</sup>

Figure 3 shows the dependence of the effective distance  $r_e$  on the Onsager radius  $r_c$  at different screening lengths. It is readily seen, that the derivative of the curves as  $r_c / \sigma \rightarrow 0$  is different if  $E$  is less or larger than 1. Indeed, the Lambert  $W$  function at small values of its argument may be expanded to give

$$W_L(x) \approx x \quad x \ll 1 \quad (5.4)$$

or

$$\frac{r_e}{\sigma} \approx \frac{r_c}{\sigma} E \frac{e^{1/E}}{(1+E)} \quad \text{for} \quad \frac{r_c}{\sigma} \frac{e^{1/E}}{(1+E)} \ll 1 \quad (5.5)$$

At  $E \lesssim 1$  the derivative becomes large and  $E$ -dependent, while for  $E \gg 1$  it tends to 1 (see Figure 3).

The Coulomb interactions affect both the forward and backward electron transfer, changing free energies (2.2) and (2.5) and the trajectories of reactant motion in the electrostatic potentials. In both reactions I and II,  $\Delta G$  for the forward electron transfer increases due to Coulombic interactions but decreases for backward electron transfer. The effect of the reactant motion in the electrostatic field is also quite transparent. The repulsive interactions reduce the total residence time in the reaction layer

and thus reduce the efficiency of the electron transfer. Attractive interactions yield the opposite effect, increasing the efficiency of the electron transfer between counterions. However, the influence of the repulsive Coulomb interaction on the initial RIP distribution has to be discussed further, in the context of the qualitatively different experimental results obtained for reactions I and II.

In the kinetic (fast diffusion) limit, the shape of the initial RIP distribution coincides with the shape of the forward-transfer rate, provided there is no Coulombic interaction. At  $|\Delta G_r| > |\Delta G_i|$  the reaction layer for backward electron transfer is more remote than for the forward one. Therefore, the ions produced by kinetic controlled forward transfer start from inside the recombination layer. According to what is known for inner starts<sup>2,15</sup> there should be a descending dependence of the recombination efficiency parameter  $Z$  on diffusion. However, in reaction I only the ascending dependence  $Z(\bar{D})$  was observed (Figure 2).<sup>17</sup> The paradox might be resolved if a repulsive Coulomb interaction strongly affects the shape of the initial distribution  $f(r)$ , making it more remote than the recombination layer. This can change the viscosity dependence of  $Z$  to the opposite, specific to reaction II in highly viscous solvents (Figure 2). However,  $f(r)$  is rather weakly affected. The layer for the low exergonic forward electron transfer is very narrow. The repulsive Coulomb forces reduce the probability of approaching this layer, but leave the spatial distribution in the donor–acceptor pair to be smooth. After normalization this distribution acquires almost the same shape as in the absence of any electrostatics. The difference between reactions I and II should be explained another way.

## VI. Charge Separation Quantum Yield

It turns out, that the main difference between these reactions does not originate from the electrostatic interaction of reactants. Neither does it arise from their spin states. They can affect the slope of  $Z(\bar{D})$  dependence only in reaction I, which can be controlled by spin conversion,<sup>19,20</sup> but not in reaction II where the slope nevertheless actually changes the sign. Only the energetics of electron transfer is essential in the reactions being compared. The free energies of transfer determine the Arrhenius factors in eqs 2.1 and 2.3 as well as the shape of the transfer rates, which deviate from the universal exponential space dependence of the tunneling factor. If the free energies of ionization and recombination are the same (as well as other parameters), then the shape of both reaction layers is also the same although different from the exponential (Figure 4a). However, if  $|\Delta G_r|$  exceeds  $|\Delta G_i|$ , then recombination becomes more remote than ionization (Figure 4b).

Whatever are the rates for forward and backward transfer, the descending  $Z(\bar{D})$  dependence can never be obtained if they are the same. In this case the initial charge distribution is always more remote than the reaction zone, so that ions enter it from outside. The common demerit of contact and exponential approximations is the identical shape of both reaction layers, for forward and backward transfer. Only the Marcus rates are free from such a drawback because they include the space dependent Arrhenius factors that make them different for ionization and recombination. The former becomes sharper than the latter if ionization free energy is less than recombination one. This difference provides the conditions for emergence of descending  $Z(\bar{D})$  dependence peculiar to inner starts.

Since in reaction II the free energy for backward transfer is larger than in reaction I, the recombination layer in the former case is shifted farther from contact than in the latter. At even

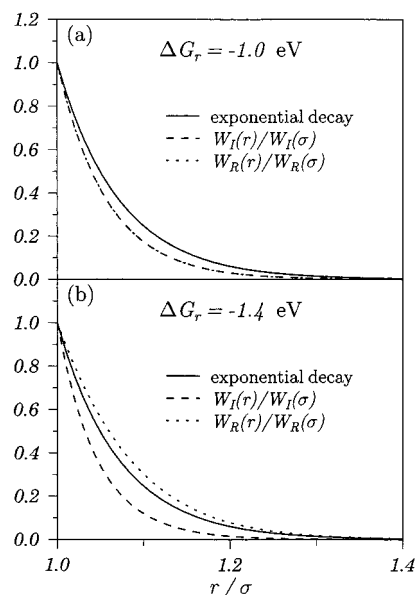


**Figure 4.** Shapes of the Marcus-type rates of forward ( $W_I$ ) and backward ( $W_R$ ) transfer in a highly polar solvent ( $\epsilon_c = 0$ ), compared to their exponential tunneling factor (solid line). The recombination free energy is either equal to that of ionization (a), or larger than it (b), provided that the excitation energy of the donor  $\mathcal{E} = 2$  eV is the same in both cases. The other parameters:  $i_1 = 0.2$  eV,  $i_0 = 1.0$  eV, preexponential factors  $w_1 = w_R = 100$  ns<sup>-1</sup>,  $L = 1$  Å,  $\sigma = 7$  Å.

higher exergonicity of transfer the recombination layer acquires a bell shape with the maximum shifted rather far.<sup>2</sup> Using a rectangular model for such a bell-shaped layer, it has been demonstrated that  $Z(D)$  crucially depends on whether the starting distance  $r$  lays inside or outside this layer.<sup>16</sup> Even not coming to such an extreme, one can get the qualitatively different  $Z(D)$  dependence for inner and outer starts. The fact that this alternative has not been discovered so long results from the identity of transfer rate shapes in all models except the rectangular one. The comparison made below between IET results and these crude models demonstrates their deficiency in accounting for such a fine feature of the phenomenon.

**A. Contact Approximation.** If electron transfer proceeds in the normal Marcus region, its rate sharply decreases with distance and is often approximated by the  $\ddot{a}$ -function located at the contact:

$$W(r) = \frac{k}{4\ddot{\sigma}r^2} \ddot{a}(r - \ddot{\sigma}) \quad (6.1)$$

Here  $k = k_0$  is the kinetic rate constant for the forward transfer and  $k = k_c$  for the backward one:

$$k_0 = \int W_I(r) d^3r \quad \text{and} \quad k_c = \int W_R(r) d^3r \quad (6.2)$$

The contact approximation for forward transfer was coming into use from the pioneering works of Smoluchowski<sup>34</sup> and Collins–Kimball.<sup>35</sup> The vast majority of analytic results for geminate recombination were also obtained with this very approximation.<sup>36–41</sup>

In the contact approximation, the initial distance between ions  $r_0$  is greater than or equal to  $\ddot{\sigma}$ . The quantum yield of their separation sharply depends on it.<sup>36,37</sup>

$$\alpha(r_0) = \frac{1 + (k_c/4\bar{\delta}r_c\bar{D})e^{r_c/\bar{\delta}}[e^{-r_c/r_0} - e^{-r_c/\bar{\delta}}]}{1 + (k_c/4\bar{\delta}r_c\bar{D})[e^{r_c/\bar{\delta}} - 1]} = \frac{1}{1 + Z(r_0)/\bar{D}} \quad (6.3)$$

It is different for the slow and fast diffusion limits:

$Z =$

$$\begin{cases} \frac{q}{1-q}\bar{D} & \text{diffusional geminate recombination } \bar{D} \ll (1-q)z \\ qz & \text{kinetic geminate recombination } \bar{D} \gg (1-q)z \end{cases} \quad (6.4)$$

where

$$q = \frac{1 - \exp(-r_c/r_0)}{1 - \exp(-r_c/\bar{\delta})} \quad z = \frac{k_c}{4\bar{\delta}r_c} (e^{r_c/\bar{\delta}} - 1)$$

In the kinetic limit, the recombination efficiency  $Z = qz$  is constant like in the primitive “exponential model” prescribing  $r = \bar{\delta}$  and  $Z = z = \text{const}$  (Figure 5). Contrary to this, in the diffusional limit  $Z$  increases linearly with  $\bar{D}$  because diffusion accelerates the delivery of ions from the place where they were born to the contact reaction zone. Due to this linearity, the charge separation quantum yield (6.3) is constant under the diffusional control of geminate recombination:

$$\alpha(r_0) = \frac{\exp(-r_c/r_0) - \exp(-r_c/\bar{\delta})}{1 - \exp(-r_c/\bar{\delta})} \quad (6.5)$$

This is a case where the exponential model and contact approximation disagree qualitatively and the choice between them can easily be made experimentally. For instance, the authors of ref 42 studied the viscosity dependence of photocurrent  $i$ , which is a product of ion mobility  $\bar{i} \propto \bar{D}$  and ion concentration  $n \propto \bar{\alpha}$ . It was found that  $i = e\bar{i}n$  is linear in the inverse viscosity  $1/L \propto \bar{D}$ . Hence, this is mobility that is responsible for the obtained linearity of  $i(\bar{D})$  dependence, provided  $n$  and  $\bar{\alpha}$  do not depend on diffusion. The last condition is met only under diffusion control of recombination.

The fact that geminate recombination in reaction I is accelerated by diffusion was first established experimentally in ref 17 and attributed to the diffusional control of this reaction in ref 14. The deviation from linear  $Z(\bar{D})$  dependence caused by an external magnetic field was later explained as mixed diffusion and spin-conversion control of geminate recombination.<sup>19,20</sup> The spin transitions, initially converting created triplet RIPs to singlet ones, allow their recombination to the ground state. Both diffusional and magnetic field effects are available for the analytic investigation in the contact approximation used for this goal in refs 40 and 41.

However, due to the weak exergonicity of the forward transfer, its rate is too small. When studied in low viscosity solvents, the forward transfer is rather kinetic than diffusional and creates only contact RIPs whose recombination cannot be accelerated by diffusion. An alternative explanation of the experimentally observed acceleration will be given in section VII. Since in reaction II the forward transfer is more exergonic, it is faster. When studied in solvents of higher viscosity, it is actually under diffusional control, as well as the subsequent recombination of RIPs. However, the recombination in reaction II is more exergonic and therefore noncontact, which makes the contact approximation inapplicable to it in less viscous solvents.

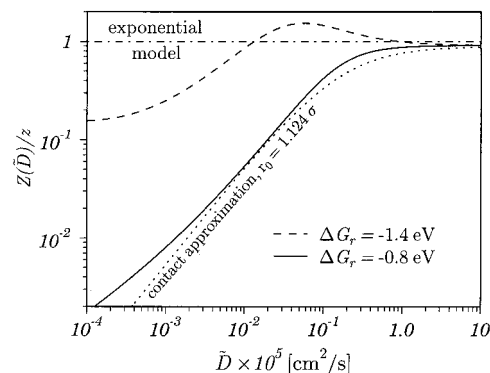


**Figure 5.** Diffusional dependence of the recombination efficiency  $Z$ , in the contact approximation (dotted line) at starting distance  $r_0 = 1.124\bar{\delta}$  and the same for the remote recombination in a normal (solid line) and inverted (dashed line) Marcus region, in highly polar solvents. The horizontal dashed–dotted line represents the exponential model result,  $Z = z = \text{const}$ .

In any case we need more consistent analysis of the recombination efficiency than that available in the contact model. The latter leaves  $k_c$  and  $r_0$  free as the fitting parameters. The proper choice of  $r_0$  brought closer together the results obtained with this approximation and IET, provided  $k_c$  is obtained from eq 6.2 and  $r_0$  is large enough. However, the similarity takes place only in the intermediate, diffusion controlled and far kinetic regions (solid and dotted lines in Figure 5). In the static limit (at  $\bar{D} \rightarrow 0$ ) the true  $Z$  is again constant although much smaller than  $qz$ . The corresponding IET value of the quantum yield is zero:  $\lim_{\bar{D} \rightarrow 0} \bar{\alpha} = 0$ , while the contact estimate (6.5) remains finite. This is an evident deficiency of the contact approximation. In fact, the remote backward transfer kills all immobile RIPs wherever they are, while recombination at contact can do nothing, if the remote ions do not move. At larger  $|\Delta G_r|$  the deviations from the contact approximation are more pronounced and not only at slow diffusion, but also in the opposite limit where the IET curve passes through the maximum, which is a new feature of the phenomenon (dashed line in Figure 5). This maximum, which will be discussed below, was really obtained experimentally and well fitted recently by means of IET.<sup>43</sup>

**B. Exponential Approximation of Transfer Rates.** Even at fast diffusion the contact approximation is useless if recombination is remote. Only encounter theory of distant transfer accounts properly for distant transfer whose rate is usually assumed to be exponential. For a long time this was a very popular simplification.<sup>7,19,44–46</sup> It results from a simple replacement  $\Delta G_I(r) \rightarrow \Delta G_I$ ,  $\Delta G_R(r) \rightarrow \Delta G_R$ , and  $\bar{i}(r) \rightarrow \bar{i}(\bar{\delta})$  in transfer rates (2.1) or (2.3), which ignores the space dependence of their Arrhenius factors:

$$W_{I,R}(r) \approx W_{I,R}(\bar{\delta}) \exp\left(-\frac{2(r-\bar{\delta})}{L}\right) \quad (6.6)$$

The variation of free energies does not change the shape of the rates affecting only their preexponential factors. As far as the rates of the forward and backward transfer have the same shape as in Figure 4a, the recombination can only be accelerated by speeding up the encounter diffusion. As a result, there should be no extremum in all curves  $Z(\bar{D})$  calculated in the exponential approximation. To prove this expectation, we have to compare the results obtained with the exact Marcus rates and their exponential simplification (6.6). The pre-exponents in eq 6.6 are chosen from the relationship

$$W_{\text{LR}}(\bar{\sigma}) \int_0^\infty \exp\left(-\frac{2(r-\bar{\sigma})}{L}\right) d^3r = \int_0^\infty W_{\text{LR}}(r) d^3r$$

to have the same kinetic limit at  $D = \bar{D} \rightarrow \infty$  as from the real transfer rates  $W_{\text{LR}}(r)$ . In Figure 6 the charge separation quantum yield  $\bar{\alpha}$  is shown as a function of the encounter diffusion coefficient in its realistic range  $10^{-7} \leq \bar{D} \leq 10^{-4}$  cm<sup>2</sup>/s. It is seen readily that at slow diffusion there appears a significant deviation between the curves calculated for the realistic Marcus-type rates and for their exponential approximations. When ionization is more exergonic, than recombination, the exponential approximation leads to some underestimation of the quantum yield, while in the opposite case it overestimates  $\bar{\alpha}$ .

**C. Nonmonotonous  $Z(D)$  Dependence in IET.** These small differences become of principal importance when one turns from the quantum yield (Figure 6) to the recombination efficiency (Figure 7). All dashed curves representing the exponential model of transfer rates monotonically increase, approaching the kinetic limit from below. As to the exact results, they are the same only for the lowest recombination free energy  $\Delta G_r = -0.8$  eV represented by the lowest curve in Figure 7. Two other curves calculated with the Marcus rates pass through the maxima and approach the kinetic limit from above. This is the most thin feature of the phenomenon.

Both the exponential and contact approximations provide only the monotonic increase of  $Z$  with  $\bar{D}$ . This is consistent with the ascending branch of the whole curve, but not with descending one, which is of a different origin. It was shown by the example of a rectangular model of  $W_{\text{R}}(r)$  that the ascending branch describes the recombination of RIPs when they start from outside the reaction layer, while the descending branch appears when the start is taken from inside.<sup>2,16</sup> The encounter diffusion helps radical ions that start from outside the recombination layer to reach and enter it. In the contact approximation this may be considered as geminate recombination under diffusional control, eq 6.4. But the same diffusion assists those RIPs that were born or brought inside the remote recombination layer to escape from it. The faster it is, the shorter is the residence time inside the reaction layer and the smaller the efficiency of recombination. In this way diffusion accelerates the recombination of outer particles and decelerates the recombination of inner particles, resulting in a two-branch nonmonotonic  $Z(\bar{D})$  dependence.

The position of the maximum and the very existence of it on the curve  $Z(\bar{D})$  depends on the relationship between the free energies of the forward and backward electron transfer. If  $|\Delta G_{\text{R}}| > |\Delta G_{\text{I}}|$  with all other parameters remaining the same, the recombination layer is wider than the ionization one, due to the space dependence of the Arrhenius factors in eqs 2.1 and 2.3. In the opposite case, at  $|\Delta G_{\text{R}}| < |\Delta G_{\text{I}}|$ , the ionization layer is wider so that the forward transfer always takes place outside the recombination layer. This situation is favorable for the contact approximation, but rarely possible.

As a rule, backward transfer is more exergonic than forward transfer and therefore more remote than  $W_{\text{I}}(r)$ . The latter determines the shape of the initial RIP distribution, which nears contact as the diffusion increases and finally coincides in shape with  $W_{\text{I}}(r)$ .<sup>2</sup> In this (kinetic) limit the majority of RIPs appear closer to contact than the recombination layer and should cross it when separated. This is represented by the descending branch of the  $Z(\bar{D})$  curve following an ascending one.<sup>15</sup> The ascending branch first obtained in ref 17 was attributed to the diffusion controlled recombination of RIPs created far away.<sup>14,19,20</sup> The opposite behavior and the maximum between the two branches,

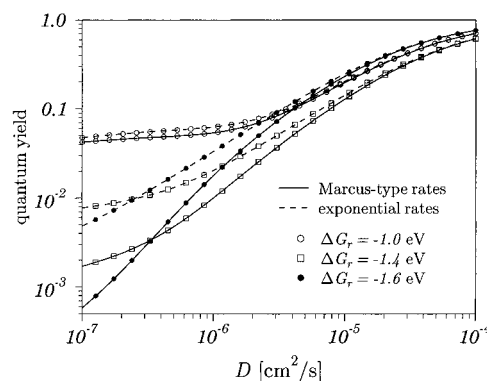


**Figure 6.** Quantum yield of the photochemical charge separation at different exergonicities of the backward electron transfer. The solid lines correspond to the Marcus-type rates, while the dashed lines, to their exponential approximations. The other parameters are the same as for Figure 4.

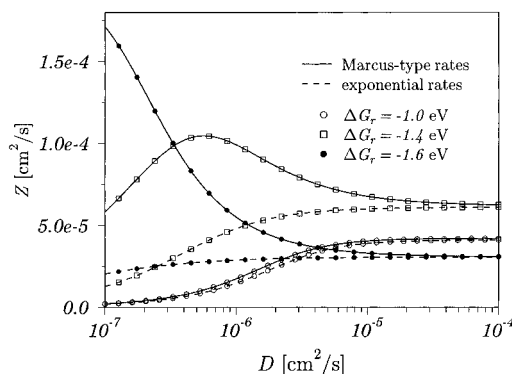


**Figure 7.** Recombination efficiency parameter  $Z$  extracted from the corresponding charge separation quantum yield, represented in Figure 6.

was only recently observed experimentally by Angulo and Grapp and well fitted by means of IET in our latest work.<sup>15</sup>

## VII. Changing of Macroscopic Parameters in Solutions

Thus, the main question that should be answered is why the maximum of  $Z$  and its descending branch, discovered in reaction II, were not achieved in reaction I. To resolve this paradox, one should take into account that the viscosity of the solution is usually varied by changing solvents or the composition of their mixtures. Apart from the viscosity, some macroscopic parameters of the mixture are also changing. These are the dielectric constant and refraction index  $n$ . Variation of  $n$  changes the Onsager radius as well as the residence time in the recombination layer. What is even more important, the variation of  $n$  and  $\epsilon$  affects the outer-sphere reorganization energy, through its contact value  $\dot{\lambda}_0$  defined in eq 2.7. As a result the total reorganization energy (2.6) changes with the composition of the solvent, together with its viscosity. In other words  $\dot{\lambda}(r)$  depends on  $\bar{D}$ , although this important factor was never taken into account. Meanwhile, the inverted region becomes normal with increasing  $\dot{\lambda}_0$ , making remote recombination contact. With a moderate increase of  $\dot{\lambda}$ , less dramatic changes occur, but still the maximum of the  $Z(\bar{D})$  curve shifts to a higher  $\bar{D}$  and can be driven out of the available viscosity interval.

As was stated, the efficiency of the ion recombination in reaction I, studied experimentally in ref 17, was found to increase monotonically with diffusion (see triangles in Figure 2). However, this dependence cannot originate from "outer" starts. With the exergonicities of electron-transfer specific to

this system ( $\Delta G_r = -1.7$  eV,  $\Delta G_i = -0.33$  eV), the recombination layer is more remote than the ionization layer, as can be seen in Figure 4b. This leads to “inner” starts at fast diffusion, because the initial RIP distribution in this limit reproduces the ionization layer, which is much sharper. At such starts,  $Z$  is expected to decrease with diffusion, but the observed  $Z(\bar{D})$  dependence in reaction I is the opposite. Since the recombination of contact born RIPs cannot be diffusional, there should be an alternative explanation for this dependence. We believe that a similar dependence may be attributed to reinforcement of the recombination with an increase in the outer-sphere reorganization energy in solvent mixtures of lower viscosity.

To prove this statement, we made another attempt to fit the experimental results of ref 17 by taking into account the reorganization energy changing. For our numerical simulations we used the following set of parameters, listed in ref 17: the free energies of electron transfer,  $\Delta G_i = -0.33$  eV and  $\Delta G_r = -1.7$  eV; inner-sphere reorganization energy,  $i = 0.3$  eV; ionic strength of the solution,  $i = 0.2$  M; the radii of reactants,  $r_1 = 6$  Å (for the Ru complex) and  $r_2 = 4$  Å (for  $MV^{2+}$ ), which constitute the contact distance  $\delta = r_1 + r_2 = 10$  Å. From this set of data we calculated the following parameters:

$$i_D = 2.38 \sqrt{\text{Å}} \quad i_0 = 1.56\zeta [\text{eV}]$$

$$r_c = q_1 q_2 570.3 / [\text{Å}] \quad (7.1)$$

The Stokes–Einstein relationship was used to express the diffusion coefficient through the viscosity of the solvent:

$$\bar{D} [\text{cm}^2/\text{s}] = 0.894 \times 10^{-5} / \eta [\text{cP}] \quad (7.2)$$

All other parameters changing with viscosity, including Pekar’s factor  $\zeta = (1/\epsilon_0 - 1/\epsilon)$ , were borrowed or calculated from the same data sources<sup>17</sup> and placed in the following table:

$\eta$ , cP	0.834	1.295	2.15	3.884	7.68	13.4
$n$	1.347	1.365	1.382	1.40	1.416	1.427
$\epsilon$	57.8	53.5	49.1	44.8	40.5	38.3
$\zeta$	0.5338	0.518	0.503	0.488	0.474	0.465

Thus, the medium dielectric constant is varied by 40%, while Pekar’s factor  $\zeta$  is changed by 14% in the whole range of available viscosities. The change in  $\epsilon$  affects the Coulomb interactions in the  $[\text{Ru}^{3+} \cdots \text{MV}^+]$  pair, while the change in  $\zeta$  affects the outer-sphere reorganization energy. The viscosity dependence of both  $\epsilon$  and  $\zeta$  is well interpolated by the two-exponential model function

$$y(\eta) = y_0 + ae^{-(\eta-L_0)/x_1} + be^{-(\eta-L_0)/x_2} \quad (7.4)$$

with the following parameters.

$y_0$	$a$	$b$	$L_0$	$x_1$	$x_2$
36.2	11.98	11.69	0.627	1.21	7.33
$\zeta$	0.457	0.04	0.046	0.606	0.98
					7.38

The accuracy of interpolation is demonstrated in Figure 8. Using the interpolations, given by eqs 7.1–7.5, we were able to get smooth curves that well approximate the experimental data in the whole region of interest.

Only three parameters were varied to fit the diffusional dependence of  $Z$ : the pre-exponents of the transfer rates for the forward and backward transfer,  $w_f$  and  $w_r$ , and the decay length of tunneling,  $L$ . A good fit (solid line in Figure 9) was obtained at rather realistic values:  $w_f = 10^3$  ns<sup>-1</sup>,  $w_r = 1.1 \times 10^3$  ns<sup>-1</sup>, and  $L = 1.35$  Å. If  $\zeta$  and  $\epsilon$  were not changed with the

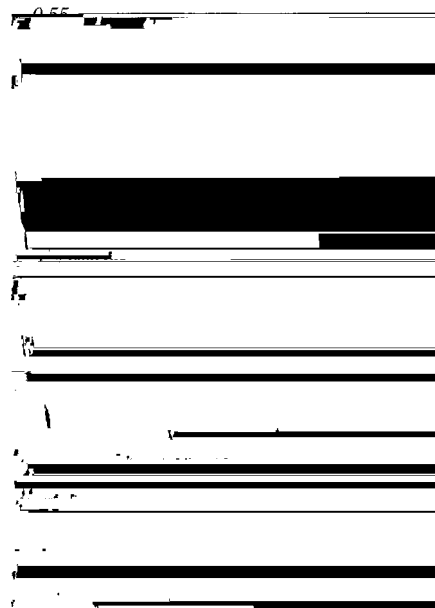


**Figure 8.** Experimental dependences of Pekar’s factor (a) and the dielectric constant (circles) on the viscosity and their interpolations by eqs 7.4–7.5.

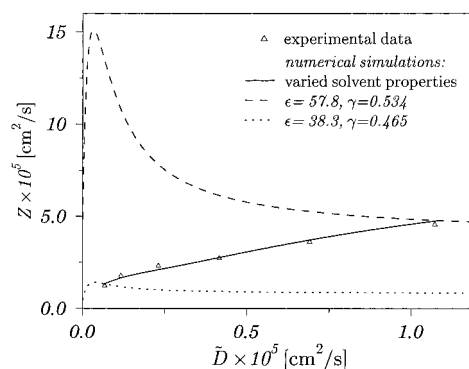


**Figure 9.** Dependence of the recombination efficiency parameter  $Z$  on the diffusion coefficient  $\bar{D}$ . The experimental data are shown by symbols (triangles). The solid line corresponds to the calculation, when the change in dielectric constant and refraction index  $n$  along with diffusion was taken into account. The dashed line corresponds to the calculation with fixed  $\epsilon = 57.8$  and  $n = 1.347$  (these values in the experiment are reached at fastest diffusion  $\bar{D} = 1.072 \times 10^{-5}$  cm<sup>2</sup>/s). The dotted line corresponds to the fixed  $\epsilon = 38.3$  and  $n = 1.427$  (slowest diffusion  $\bar{D} = 6.67 \times 10^{-7}$  cm<sup>2</sup>/s).

solvent viscosity (diffusion), the result would be qualitatively different. To illustrate this point, we performed two other calculations with invariable  $\zeta$  and  $\epsilon$ . One time their values were fixed, equal to those that correspond to the slowest diffusion ( $\bar{D} = 6.67 \times 10^{-7}$  cm<sup>2</sup>/s,  $\epsilon = 38.3$ ,  $\zeta = 0.465$ ), while another time, conversely, they were the same as for fastest diffusion ( $\bar{D} = 1.072 \times 10^{-5}$  cm<sup>2</sup>/s,  $\epsilon = 57.8$ ,  $\zeta = 0.5338$ ). In Figure 9, the former is shown by a dotted line and the latter by a dashed one. It can be seen readily that both curves calculated at fixed  $\zeta$  and  $\epsilon$  pass through the maximum and their viscosity dependence at faster diffusion is the opposite of that obtained experimentally. The ascending branches of these curves can be attributed to the diffusion delivery of remote RIPs into the recombination zone, as was stated in refs 19 and 20. However, this is not an explanation of the  $Z(\bar{D})$  dependence for reaction I, as we thought previously. All experimental data for this reaction lie in the range of relatively fast diffusion, when the forward electron transfer is under kinetic control. Such a transfer

produces an initial RPs distribution nearest to contact and almost invariable with further diffusion acceleration (Figure 10a). Moreover, their sensitivity to the electrostatic interaction of reactants is very weak, as was stated in section V. The RPs do not draw significantly back from contact due to repulsion, and they are from the very beginning almost completely inside

- (29) Lukzen, N. N.; Krissinel, E. B.; Igoshin, O. A.; Burshtein, A. I. *J. Phys. Chem. A* **2001**, *105*, 19.
- (30) Burshtein, A. I.; Frantsuzov, P. A. *Chem. Phys. Lett.* **1996**, *263*, 513.
- (31) Burshtein, A. I.; Ivanov, K. L. *J. Phys. Chem. A* **2001**, *105*, 3158.
- (32) Burshtein, A. I.; Neufeld, A. A.; Ivanov, K. L. *J. Chem. Phys.* **2001**, *115*, 2652.
- (33) Corles, R. M.; Gonnet, G. H.; Hare, D. E. G.; Jeffrey, D. J.; Knuth, D. E. *On the Lambert W Function* Maple Share Library.
- (34) Smoluchowski, M. V. *Z. Phys. Chem.* **1917**, *92*, 129.
- (35) Collins, F. C.; Kimball, G. E. *J. Colloid Sci.* **1949**, *4*, 425.
- (36) Hong, K. M.; Noolandi, J. *J. Chem. Phys.* **1978**, *68*, 5163.
- (37) Sano, H.; Tachiya, M. *J. Chem. Phys.* **1979**, *71*, 1276.
- (38) Gözele, U. *Chem. Phys. Lett.* **1980**, *69*, 332.
- (39) Tachiya, M. *Radiat. Phys. Chem.* **1983**, *21*, 167.
- (40) Burshtein, A. I.; Krissinel, E. *J. Phys. Chem. A* **1998**, *102*, 816, 7541.
- (41) Burshtein, A. I. *Chem. Phys.* **1999**, *247*, 275.
- (42) von Raumer, M.; Sarbach, A.; Haselbach E. *J. Photochem. Photobiol. A. Chem.* **1999**, *121*, 75.
- (43) Burshtein, A. I.; Neufeld, A. *J. Chem. Phys.*, in press.
- (44) Philling, M. J.; Rice, S. A. *J. Chem. Soc., Faraday Trans. 2* **1975**, *71*, 1563.
- (45) Berlin, Yu. A. *Dokl. Akad. Nauk SSSR* **1975**, *223*, 625.
- (46) Doktorov, A. B.; Burshtein, A. I. *Sov. Phys. JETP* **1976**, *41*, 67